Properties of nanostructured Ge produced by laser-induced air breakdown processing

A. V. Kabashin,[a] F. Magny, and M. Meunier
Departement de Genie Physique, Ecole Polytechnique de Montréal, Case Postale 6079, Succursale Centre-ville, Montréal, Québec H3C 3A7, Canada

(Received 23 August 2006; accepted 11 December 2006; published online 12 March 2007)

Germanium wafers have been modified by a technique of laser-induced air breakdown processing. It has been found that the treatment leads to the formation of porous layers, containing nanoscale holes, and consists of Ge nanocrystals embedded into GeO_2 matrices. They exhibit strong and stable photoluminescence in the green and UV ranges (2.2 and 2.9 eV), whose appearance could be explained by defects in the GeO_2 matrix or quantum confinement effects. The locally patterned layers are of importance for optoelectronics and biosensing applications. © *2007 American Institute of Physics*. [DOI: 10.1063/1.2435801]

I. INTRODUCTION

Silicon and germanium are group IV semiconductors, which are of vital importance for the microelectronics industry. However, having indirect and small band gaps (1.1 eV for Si and 0.6 eV for Ge), both materials do not emit visible light, which complicates their use for optoelectronics applications. Promises for these applications arose with the observation of visible photoluminescence (PL) from anodically etched porous Si (Ref. 1) and nanostructured thin films prepared by various deposition techniques, including "dry" ones, which are compatible with semiconductor processing technologies.[2–8] Similar effect was observed with chemically etched Ge (Refs. 9 and 10) and Ge-based films.[11–13] Although the origin of visible PL has not yet been clarified, applications of nanostructured semiconductors in photonics[14] and biosensing[15] are now extensively discussed.

We recently demonstrated a simple, dry, and vacuum-free method for local nanostructuring of silicon.[16–19] The method consists of the IR laser radiation-induced initiation of air breakdown on the Si surface, while the target presence serves to decrease the threshold of the plasma initiation.[20] The hot plasma of air optical breakdown causes a modification of target material, transforming it into a porous nanostructured layer. Since main IR radiation power is absorbed by the plasma itself, radiation cannot reach the target and cause significant removal of its material. Therefore, layers produced by laser-induced air breakdown (LIAB) processing are different from structures formed by conventional laser ablation, which are characterized by a significant radiation-based removal of material and a formation of spikelike structure within the irradiation spot.[21–25] The LIAB-based treatment has been successfully applied to treat silicon wafers and produce local nanostructured spots, exhibiting strong visible PL.

In this paper, we apply the air optical breakdown technique to treat Ge and study properties of the layers formed on its surface.

[a]Electronic mail: andrei.kabashin@polymtl.ca

II. EXPERIMENT

In the experiments, the radiation from a pulsed transversely excited atomsphere (TEA) CO_2 laser [wavelength 10.6 μm, pulse energy 1 J, pulse length 1 μs full width at half maximum (FWHM), and repetition rate 3 Hz] was focused by Fresnel's lens (focal length of 5 cm) onto a Ge target. The radiation intensity was about 10^8 W/cm^2 at the focal plane. The experiment was carried out in atmospheric air (1 atm, 20 °C, 40% humidity). Standard germanium wafers (n and p types, resistances of 0.01–10 Ω cm) with dimensions of about 1×1 cm^2 were used as targets.

Scanning electron microscopy (SEM) (Phillips XL20, Phillips Corp.) was used to examine structural properties of the films. The crystalline structure of the films was studied by x-ray diffraction (XRD) spectroscopy (X'pert XRD system, Philips Corp.). The presence of nanocrystals in formed layers was examined by transmission electron microscopy (TEM) (model Philips CM30) using a cross-sectional technique. A treated sample was at first cleaved. The two halves were cemented together face to face by epoxy. The sample was mechanically grounded perpendicular to the cemented face to 100 μm thickness. One portion was mounted on a 3 mm Cu support grid and dimpled to 20 μm thickness using diamond paste. Then it was ion milled in argon to perforation. The surface analysis was performed at a base pressure below 10^{-10} Torr by the x-ray photoelectron spectroscopy (ESCALAB 3 Mark II, VG Scientific), using 1253.6 eV radiation from a Mg $K\alpha$ x-ray source. Photoacoustic Fourier transform infrared (FTIR) spectra were obtained using a He-purged MTEC 300 photoacoustic cell in a Bio-Rad FTS 3000 spectrometer. The PL spectra were measured at room temperature using a double spectrometer. The samples were illuminated by the radiation of Cd (325 nm) and Ar^+ (488 nm) lasers.

III. RESULTS

As in the case of silicon[16–19] the breakdown initiation threshold on Ge depended on the efficiency of radiation absorption by the upper target surface layer. In particular, rela-

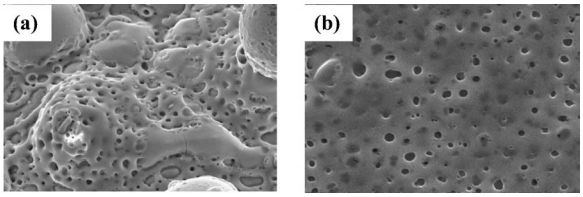

FIG. 1. SEM images of the treated Ge surface after 900 laser shots. (a) Central region, magnification of 2000× and (b) peripheral region, magnification of 5000×.

tively high radiation powers were required to ignite the breakdown on a clean Ge wafer. However, the threshold was significantly lower when the radiation spot hit dust on the wafer surface. After the breakdown ignition, the plasma intensity rose progressively with the number of laser shots on the same spot and stabilized only after 20–100 shots. The intensity gain was apparently related to the improvement of radiation absorption due to the formation of mechanical defects on the surface. In our experiments, the treatment was performed under near-threshold conditions to minimize possible deposition of material on the surrounding free target surface. After breakdown initiations by several laser pulses, a gray-tint layer was formed under the irradiation spot.

It was found that the morphology of the Ge surface after the laser irradiation was inhomogeneous. As one can see from the SEM images depicted in Fig. 1, the processed layer was relatively nonuniform, whereas in the peripheral part these structures were essentially absent. Nevertheless, the entire treated surface presented a highly porous material, containing nanoscale holes between 30 and 150 nm. It is worth mentioning that similar porous structures were observed after the breakdown treatment of silicon.

We concluded from x-ray photoemission spectroscopy (XPS) spectra that only C, O, and Ge were present in the modified surface layer. As follows from Fig. 2, the high-resolution XPS spectrum of Ge samples before the treatment was characterized by peaks at 29 and 32.5 eV, which are always assigned to the inoxidized Ge core and the natural GeO_2 oxide layer, respectively. Similar to the case of breakdown-treated Si,[19] the treatment of Ge led to the disappearance of Ge-related peak, while the oxide-related peak became stronger, suggesting that the treatment led to formation of germanium oxide (GeO_2) layer. Thus, we can conclude that the upper treated layer mainly consisted of the germanium oxide. Figure 3 shows a typical photoacoustic FTIR spectrum from the treated surface. The major vibration features observed are the following: (a) The very strong and broad band, ~3500 cm^{-1}, is assigned to bonded OH stretching vibration, while a sharp shoulder, appeared at ~3700 cm^{-1}, is usually assigned to the free absorbed OH; (b) ~2900 cm^{-1} band, which can be assigned to the C–H stretching mode associated with the CH_m groups adjacent to the OH groups; (c) ~1050 cm^{-1}, which can be attributed to Ge–O stretching, the C–O stretching mode, and Ge–OH, as well as Ge–O–C stretching is also located in this region; (d) the CH_2 chain-wagging mode progression at 1200–1350 cm^{-1}; and (e) the C–H scissors deformation mode of the CH_2 group at ~1500 cm^{-1}. Disregarding signals related to carbon contamination of samples, we may conclude from the photoacoustic study that two types of important chemical processes occur during the treatment. These are the oxidation and formation of hydroxyl groups related to Ge–O and Ge–OH stretching modes, respectively.

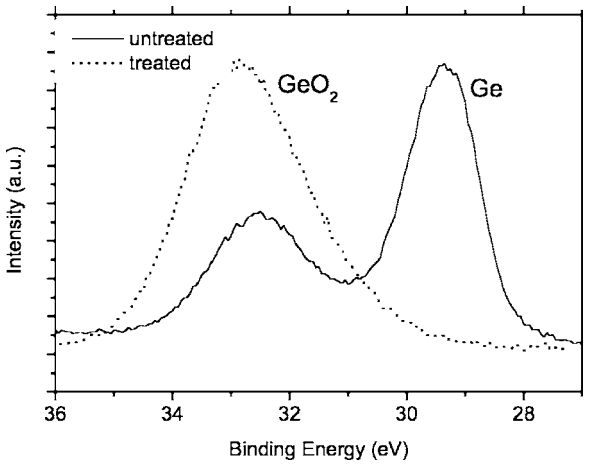

FIG. 2. High-resolution XPS spectrum from the breakdown-treated Ge surface after 900 pulses.

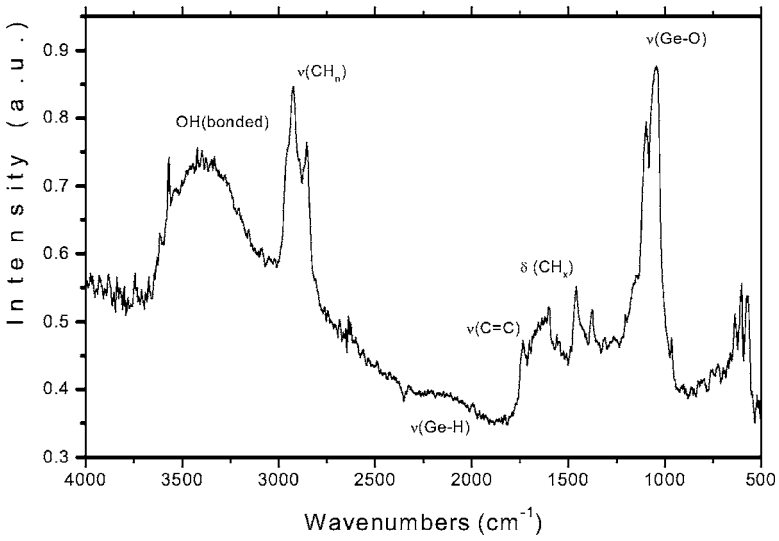

FIG. 3. Photoacoustic FTIR spectrum from the breakdown-processed Ge surface after 900 pulses.

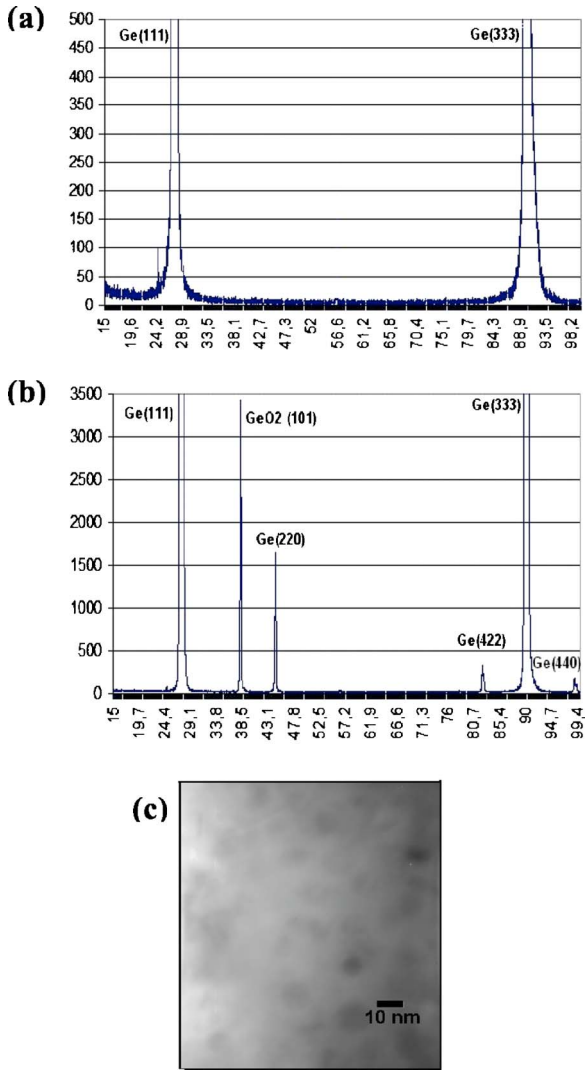

FIG. 4. Typical XRD spectra before (a) and after (b) the breakdown processing of a Ge wafer. To enhance XRD signal, a rectangular area with dimensions of 5×5 mm^2 was treated on the wafer by shifting the laser beam over the target. (c) Typical TEM image of slice of a Ge wafer near the treated area.

Nevertheless, XRD studies showed that Ge crystals are also present in the layer. Figure 4(a) shows typical spectra for a Ge target before and after the optical breakdown processing. One can see that the treatment led to the appearance of additional XRD peaks associated with different crystalline Ge states. This gives the evidence that the resulting layers consisted of Ge crystals embedded in GeO_2 matrix. The presence of nanocrystals was confirmed by TEM data. As shown in Fig. 4(c), presenting an area on a slice of treated Ge, the crystals were 10–40 nm in size, although smaller grains were also present. Notice that similar size values were obtained in the case of Si, treated by the same method.[17,18]

We found that the breakdown-processed Ge surface exhibits strong visible PL at room temperature, which is visible by a naked eye. Here, we observed two bright bands: a green one around 2.2 eV and a blue one around 2.9 eV, as shown in Fig. 5. The green signal experienced a slight decrease of its intensity under a prolonged oxidation of samples in ambient air, while the blue one was very stable. The presence of

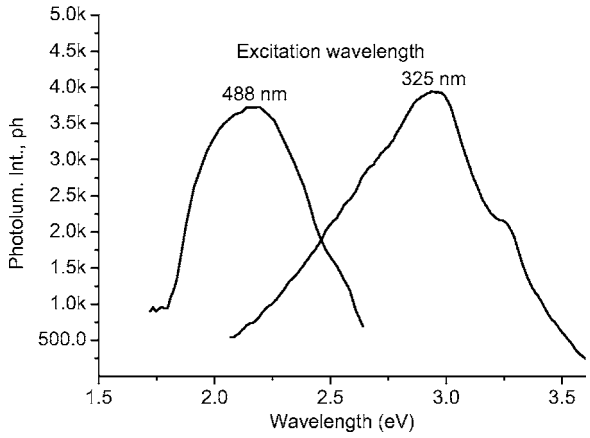

FIG. 5. Typical photoluminescence spectrum from the central part of Ge-based layer fabricated by the breakdown processing of a Ge wafer by 900 laser shots.

two bands was similar to the case of LIAB-processed Si, albeit the bands from nanostructured Si were slightly different (2.0 and 3.2 eV).[16–19] It should also be noted that electric spark processing of Ge led to the appearance of the same PL peaks around 2.2 and 2.9 eV,[26] suggesting a similar mechanism of material transformation in these two treatments.

IV. DISCUSSION

It is well known that the interaction of the CO_2 laser radiation with matter is characterized by a fast transition from a target-related to plasma-related radiation absorption.[20] The target generates initial electrons to ignite the gas discharge, which then develops into the cold gas toward the focusing lens, absorbing main IR radiation power and, as a consequence, getting heated up to high temperatures of more than 10^4 K.[20] The action of radiation probably causes a localized melting and even flash evaporation of the target material, leading to the appearance of pores on the target surface.[17] The laser-ablated material and the upper target layer are then heated by the hot CO_2 laser-induced breakdown plasma or its currents, leading to additional phase transformations and the initiation of chemical reactions. Since the radiation is pulsed, one can assume a recrystallization or local vapor redeposition of the material during the off times.

It follows from a comparison of properties of layers produced that the mechanism of air optical breakdown processing is similar in many respects to the case of the electric spark processing.[26–30] For this spark the modifications are attributed to pulsed ion bombardment of semiconductor surfaces, which led to a flash evaporation of the target material and its recrystallization during the off times. Indeed, spark-processed semiconductors also contained 10–500 nm holes and consisted of Si (Ge) nanocrystals embedded in SiO_2 (GeO_2) matrix.[26,27] Although PL properties of Si-based layers produced by these two methods could have certain differences, the Ge-based layers demonstrated similar properties with strong peaks at 2.1–2.2 and 2.9 eV. The generation of visible PL in the case of the spark-processed Ge was attributed to defects in GeO_2 structure[31] rather than to the radiative recombination of excitons confined in nanocrystals.[1]

This mechanism is also the most probable in the case of the optical breakdown processing. Indeed, plasma interaction with the Ge surface during the laser irradiation should form a large amount of defects in the oxidation layer and in the interface between the Ge core and GeO_2 oxide shell.[3] This is confirmed by the FTIR studies (Fig. 3), which gave a strong evidence for the OH absorption due to the defect-related free radicals and dangling bonds. The quantum confinement effects are less probable in the case of Ge, but they cannot be ruled out completely, taking into account that some nanocrystal sizes could be less than 5 nm (Fig. 4). In any case, more experimental data should be obtained for a clear identification of the PL origin. These studies are in progress.

V. CONCLUSION

Air optical breakdown has been produced on a Ge target to modify its surface. We showed that the breakdown production led to the formation of porous layer under the radiation spot, which consisted of Ge nanocrystals embedded in GeO_2 matrix, while its surface was characterized by the presence of oxide and hydroxyl groups. The fabricated layers exhibited strong green and blue PL, which is of importance for optoelectronics applications.

ACKNOWLEDGMENTS

The authors are grateful to D.-Q. Yang for XPS and photoacoustic FTIR measurements. They also acknowledge the financial contribution from the Natural Sciences and Engineering Research Council of Canada and the Canadian Institute for Photonics Innovations (CIPI).

[1]L. T. Canham, Appl. Phys. Lett. **57**, 1046 (1990).
[2]H. Takagi, H. Ogawa, Y. Yamazaki, A. Ishizaki, and T. Nakagiri, Appl. Phys. Lett. **56**, 2379 (1990).
[3]Y. Kanemitsu, T. Ogawa, K. Shiraishi, and K. Takeda, Phys. Rev. B **48**, 4883 (1993).
[4]I. A. Movtchan, R. W. Dreyfus, W. Marine, M. Sentis, M. Autric, G. Le Lay, and N. Merk, Thin Solid Films **255**, 286 (1995).
[5]Y. Yamada, T. Orii, I. Umezu, Sh. Takeyama, and T. Yoshida, Jpn. J. Appl. Phys., Part 1 **35**, 1361 (1996).
[6]T. Makimura, Y. Kunii, and K. Murakami, Jpn. J. Appl. Phys., Part 1 **35**, 4780 (1996).
[7]A. V. Kabashin, M. Meunier, and R. Leonelli, J. Vac. Sci. Technol. B **19**, 2217 (2001).
[8]A. V. Kabashin, J.-P. Sylvestre, S. Patskovsky, and M. Meunier, J. Appl. Phys. **91**, 3248 (2002).
[9]M. Sendova-Vassileva, M. Tzenov, D. Dimova-Malinovska, M. Rosenbauer, M. Stutzmann, and K. V. Josepovits, Thin Solid Films **255**, 282 (1995).
[10]S. Miyazaki, K. Sakamoto, K. Shiba, and M. Hirose, Thin Solid Films **255**, 99 (1995).
[11]Y. Maeda, N. Tsukamoto, Y. Yazawa, Y. Kanemitsu, and Y. Masumoto, Appl. Phys. Lett. **59**, 3168 (1991).
[12]L. Yue and Y. He, J. Appl. Phys. **81**, 2910 (1997).
[13]T. Kabayashi, T. Endoh, H. Fukada, S. Sakai, and Y. Ueda, Appl. Phys. Lett. **71**, 1195 (1997).
[14]L. Pavesi, L. Dal Negro, C. Mazzolenl, G. Franzo, and F. Priolo, Nature (London) **408**, 440 (2000).
[15]V. S.-Y. Lin, K. Motesharei, K. P. S. Dancil, M. J. Sailor, and M. R. Ghadiri, Science **278**, 840 (1997).
[16]A. V. Kabashin and M. Meunier, Appl. Surf. Sci. **186**, 576 (2002).
[17]A. V. Kabashin and M. Meunier, Appl. Phys. Lett. **82**, 1619 (2003).
[18]A. V. Kabashin and M. Meunier, Mater. Sci. Eng., B **101**, 60 (2003).
[19]D.-Q. Yang, A. V. Kabashin, V.-G. Pilon-Marien, E. Sacher, and M. Meunier, J. Appl. Phys. **95**, 5722 (2004).
[20]F. V. Bunkin, V. I. Konov, A. M. Prokhorov, and V. B. Fedorov, JETP Lett. **9**, 371 (1969).
[21]T.-H. Her, R. J. Finlay, C. Wu, S. Deliwala, and E. Mazur, Appl. Phys. Lett. **73**, 1673 (1998).
[22]C. Wu, C. H. Crouch, L. Zhao, and E. Mazur, Appl. Phys. Lett. **81**, 1999 (2002).
[23]A. J. Pedraza, J. D. Fowlkes, and D. H. Lowndes, Appl. Phys. Lett. **74**, 2322 (1999).
[24]A. J. Pedraza, J. D. Fowlkes, and D. H. Lowndes, Appl. Phys. Lett. **77**, 1629 (2000).
[25]J. D. Fowlkes, A. J. Pedraza, D. A. Blom, and H. M. Meyer III, Appl. Phys. Lett. **80**, 3799 (2002).
[26]S. S. Chang, G. J. Choi, and R. E. Hummel, Mater. Sci. Eng., B **76**, 237 (2000).
[27]R. E. Hummel and S.-S. Chang, Appl. Phys. Lett. **61**, 1965 (1992).
[28]E. F. Steigmeier, H. Auderset, B. Delley, and R. Morf, J. Lumin. **57**, 9 (1993).
[29]R. E. Hummel, A. Morrone, M. Ludwig, and S.-S. Chang, Appl. Phys. Lett. **63**, 2771 (1993).
[30]M. H. Ludwig, A. Augustin, and R. E. Hummel, Semicond. Sci. Technol. **12**, 981 (1997).
[31]S. M. Prokes, Appl. Phys. Lett. **62**, 3244 (1993).